

# Token Preference Optimization with Self-Calibrated Visual-Anchored Rewards for Hallucination Mitigation

Jihao Gu<sup>\*†1</sup>, Yingyao Wang<sup>\*1</sup>, Meng Cao<sup>2</sup>, Pi Bu<sup>1</sup>,  
Jun Song<sup>‡1</sup>, Yancheng He<sup>1</sup>, Shilong Li<sup>1</sup>, Bo Zheng<sup>1</sup>

<sup>1</sup>Alibaba Group

<sup>2</sup>Mohamed bin Zayed University of Artificial Intelligence  
{gujihao.gjh, wangyingyao.wyy, jsong.sj}@taobao.com

## Abstract

Direct Preference Optimization (DPO) has been demonstrated to be highly effective in mitigating hallucinations in Large Vision Language Models (LVLMs) by aligning their outputs more closely with human preferences. Despite the recent progress, existing methods suffer from two drawbacks: 1) Lack of scalable token-level rewards; and 2) Neglect of visual-anchored tokens. To this end, we propose a novel Token Preference Optimization model with self-calibrated rewards (dubbed as TPO), which adaptively attends to visual-correlated tokens without fine-grained annotations. Specifically, we introduce a token-level *visual-anchored reward* as the difference of the logistic distributions of generated tokens conditioned on the raw image and the corrupted one. In addition, to highlight the informative visual-anchored tokens, a visual-aware training objective is proposed to enhance more accurate token-level optimization. Extensive experimental results have manifested the state-of-the-art performance of the proposed TPO. For example, by building on top of LLAVA-1.5-7B, our TPO boosts the performance absolute improvement for hallucination benchmarks.

## 1 Introduction

Recently, Large Vision Language Models (LVLMs) have showcased their remarkable capabilities in handling multimodal information, excelling in tasks such as image captioning, visual question-answering, and complex visual reasoning (Team et al., 2023; Bai et al., 2023; Hurst et al., 2024; Yang et al., 2023). Specifically, by integrating pre-trained language models with meticulously designed visual encoders, LVLMs are capable of effectively capturing the semantic correlations between visual and textual data. This integration

<sup>\*</sup>Equal contribution.

<sup>†</sup>Work done during an internship at Alibaba Group.

<sup>‡</sup>Corresponding Author.

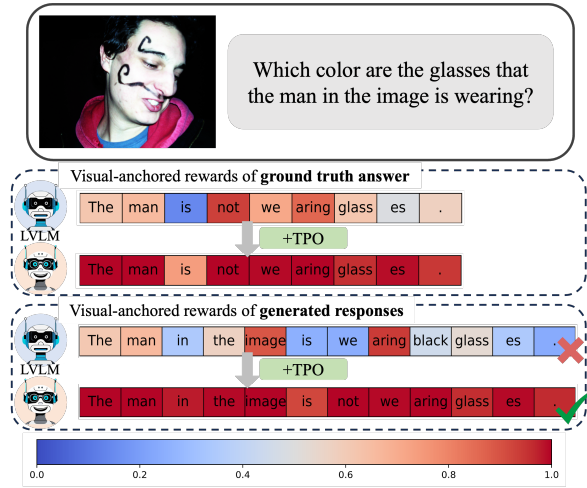


Figure 1: An example of visual Q&A. The upper box contains the ground truth answer, while the lower box shows the LVLM responses before and after training with our method. In each box, we visualize the rewards for each token which can reflect the degree of visual anchoring, with the top representing scores before training and the bottom after. Scoring is detailed in Equation 5, and we’ve applied sigmoid normalization in this score.

supports more accurate and contextually relevant tasks of visual understanding and generation.

Despite the advancements, the issue of “hallucination”, where the generated responses are not grounded in the input visual contexts, greatly impedes the reliability and practical deployment of LVLMs (Liu et al., 2024a; Bai et al., 2024). To alleviate this, various methods have been proposed from the perspectives of data quality (Liu et al., 2023; Zhai et al., 2023) and inference-time strategies (Yin et al., 2023; Zhou et al., 2023; Huang et al., 2024). Recently, direct preference optimization (DPO) (Rafailov et al., 2024) is introduced to align outputs with human preferences, therefore reducing the risk of generating hallucinatory or nonsensical responses.

Existing DPO-like methods, however, still suffer from two drawbacks: 1) *Lack of scalable token-*

*level rewards*. The fine-grained token-level rewards enable precise adjustments to individual parts of generated responses. Existing methods, however, either provide global sentence rewards or rely on manual efforts for fine-grained segment-level annotations (Yu et al., 2024b). Therefore, designing a scalable token-level reward generation strategy has become a clearly defined necessity (*c.f.* Table 1); 2) *Neglect of visual-anchored tokens*: By “visual-anchored tokens”, we refer to response tokens that are essential and highly correlated with the input visual embeddings. RLHF-V assigns all the hallucinated segments with a fixed reward value. Recent studies (Guan et al., 2024) attribute the hallucination issue to an inherent imbalance between the visual and textual modalities. Specifically, due to the large-scale pre-trained textual corpus, LVLMs tend to prioritize language-based information even at the costs of overriding the provided visual content. Therefore, we argue that not all the tokens are equal, *i.e.*, visual-anchored tokens (*e.g.*, glass in Figure 1) are more prone to hallucination and deserve great emphasis. As shown in Table 1, the concurrent pre-print V-DPO (Xie et al., 2024) also focuses on visual-anchored tokens; however, it requires the additional construction of a synthetic dataset, whereas our method eliminates the need for any extra annotations.

To alleviate these aforementioned problems, we propose a novel **Token Preference Optimization** with self-calibrated rewards (dubbed as **TPO**), which rectifies the fine-grained token-level hallucinations and attends to visual-anchored tokens without the need of fine-grained annotations. Specifically, to mine the visual-anchored tokens, we compute the differences between the logits distributions of generated tokens conditioned on the raw image and the corrupted one. We regard this distribution difference as token-wise rewards. In Figure 1, we apply this visual-anchored score mining strategy on both golden truth and the generated responses. As shown, this strategy effectively helps highlight visual-anchored tokens. Then, we propose a token preference optimization loss by integrating the self-calibrated rewards into the vanilla DPO. In particular, we multiply the like-hood distribution with token-wise rewards to generate our desired visual-correlated ones.

Overall, the main contributions of this work are:

- We propose TPO for hallucination mitigation in LVLMs, which implements token-level distribution rectification without the reliance of fine-

Methods	Visual-Anchored	Token-level	Fine-grained Annotations
DPO	✗	✗	✗
POVID	✗	✗	✗
CSR	✓	✗	✗
RLHF-V	✗	✓	✓
V-DPO	✓	✓	✓
<b>TPO (Ours)</b>	✓	✓	✗

Table 1: Comparisons with hallucination mitigation methods from the perspective of whether attending to vision-anchored tokens, whether generating token-level rewards and whether requiring fine-grained annotations. The compared methods include DPO (Rafailov et al., 2024), POVID (Zhou et al., 2024a), CSR (Zhou et al., 2024b), RLHF-V (Yu et al., 2024b), V-DPO (Xie et al., 2024) and our proposed TPO.

grained manual annotations.

- We mine visual-anchored tokens by comparing the response distributions conditioned on the raw image and the corrupted one.
- Extensive experiments on the popular hallucination benchmarks demonstrate the state-of-the-art performance of the proposed TPO.

## 2 Related Works

### 2.1 LVLMs’ Hallucination

Leveraging the rich knowledge in large language models and the vision understanding capabilities of vision encoders, LVLMs have shown exceptional performance in image understanding and generation tasks (Li et al., 2023b; Zhu et al., 2023). However, imbalances in parameters and data scale during pre-training can lead to LVLMs being overly influenced by biases in the language model, resulting in inadequate attention to visual information and potential hallucination issues (Zhou et al., 2023; Zhang et al., 2024). Consequently, addressing the issue of hallucinations in LVLMs has become one of the key research focuses in this field.

Previous studies have mitigated hallucinations by enhancing training data quality, refining decoding strategies, and post-processing generated responses (Huang et al., 2024; Leng et al., 2024; Yu et al., 2024a; Han et al., 2024; Chen et al., 2024; Zhou et al., 2023; Yin et al., 2023; Lee et al., 2023; Xia et al., 2024; Shao et al., 2024). While these methods can lead to more accurate responses, they do not fundamentally resolve the issue of inadequate visual information association in LVLMs.

## 2.2 Preference Learning Methods

More recently, reinforcement learning from human feedback (RLHF) (Sun et al., 2023) is gradually becoming a prevalent approach to mitigate the hallucination. As a more direct and effective method, DPO (Rafailov et al., 2024) and its variants are more widely utilized for preference alignment.

Several studies based on DPO focus on developing more robustly constructed preference data. For example, the POVID (Zhou et al., 2024a) method constructs negative samples for preferred data by adding noise to the image and providing hallucinated patterns to guide the model to generate hallucinated responses. The pre-structured data will be employed for off-policy DPO training. Apart from these works, RLAIIF (Yu et al., 2024c) and CSR (Zhou et al., 2024b) methods, which are built upon on-policy DPO strategy, construct preference pairs by iteratively performing self-rewarding to select preference pairs. A notable commonality among the aforementioned studies is that assigning response-level rewards for each generated sequence is insufficient for effectively aligning with genuinely hallucination-prone contents.

Other studies, RLHF-V (Yu et al., 2024b) and V-DPO (Xie et al., 2024), investigated this issue and achieved more fine-grained alignment of preference data. Nevertheless, this approach depends on resource-intensive annotations or data constructions and applies a fixed reward to all hallucinated segments, thus failing to account for the differing levels of relevance these segments may have to visual information. It is worth mentioning that CSR also considered this problem and introduced CLIP (Radford et al., 2021) to calculate the relevance score between generated text and vision information as an additional reward. However, this method requires the introduction of an additional model, which reduces the training efficiency.

In this paper, we propose a token-level preference optimization method with self-calibrated visual-anchored rewards (TPO), aimed at addressing the aforementioned challenges. TPO facilitates finer-grained alignment in LVLMs, enhancing accuracy in visual information correlation and reducing hallucinations during response generation.

## 3 Methodology

### 3.1 Motivation

As illustrated in Figure 1, the generation of each token requires differing levels of integration with

visual information. Tokens that are closely correlated with visual inputs are designated as "visual-anchored tokens" in this paper. It is observed that the generation of such visual-anchored tokens can be more susceptible to hallucinations. Furthermore, directly assigning rewards to entire generated sequences can lead to tokens independent of visual information consuming undue optimization resources. This misallocation can reduce the supervisory focus on visual-anchored tokens. To enhance training efficiency and ensure the model attends to relevant visual features, it is crucial to assign token-level rewards based on the reliance on visual information during training.

To achieve these goals, the proposed TPO mitigates hallucination from the following three key aspects: 1) scalable token-level rewards to optimize alignment; 2) automatic identification of visual-anchored tokens by the model itself; 3) self-calibration of reward signals based on visual correlation.

### 3.2 Preliminaries

DPO (Rafailov et al., 2024) is designed to directly maximize the reward margin between positive and negative responses to align human preferences. Specifically, given a textual input  $x$ , a visual input  $v$ , a negative response  $y_l$ , and a preferred positive response  $y_w$ , the reward function is defined as  $r(x, v, y_l/y_w)$ . According to the Bradley-Terry (Bradley and Terry, 1952) model, the probability of each response is as follows:

$$p(y_w > y_l) = \sigma(r(x, v, y_w) - r(x, v, y_l)) \quad (1)$$

where the sigmoid function is denoted as  $\sigma(\cdot)$ .

In this paper, we focus on the off-policy DPO method, where the probability of preference data is derived from the optimal policy rather than the reward model. The reward function is designed as:

$$r(x, v, y) = \beta \log \frac{\pi_\theta(y|x, v)}{\pi_{\text{ref}}(y|x, v)} \quad (2)$$

In Equation (2), assuming a response  $y \in \{y_w, y_l\}$  has  $N$  tokens  $(y_1, \dots, y_i, \dots, y_N)$ , the output distribution of the current policy model  $\pi_\theta(y|x, v)$  and the reference model  $\pi_{\text{ref}}(y|x, v)$  can be expressed as  $\prod_{y_i} p(y_i|x, v)$ . On this basis, the formulation of

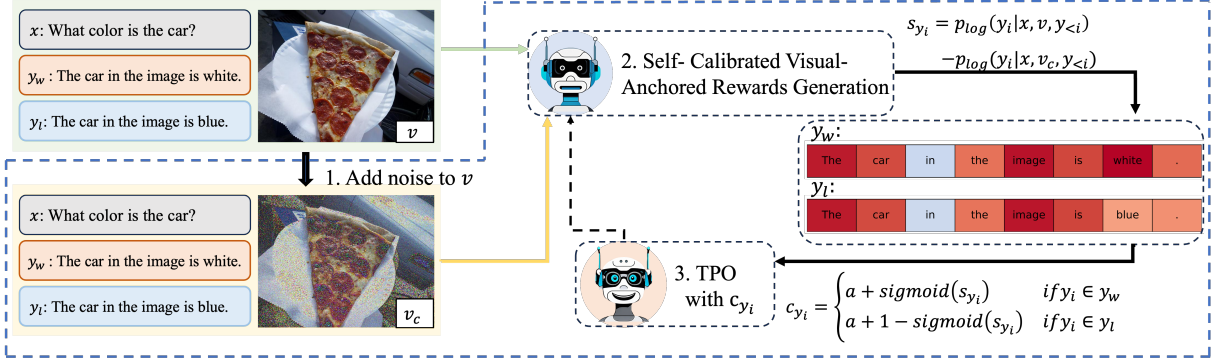


Figure 2: Outline of our TPO pipeline. The process is divided into three parts for each data at every training step. First, 1) add noise to the image, then, 2) calculate Self-Calibrated Visual-Anchored Rewards, and finally 3) perform Token Preference Optimization. At the end of each training step, we calibrate the model and calculate new Visual-Anchored Rewards for the next step.

a maximum likelihood objective is defined as:

$$\mathcal{L}_{DPO}(\pi_\theta; \pi_{\text{ref}}) = -\mathbb{E}_{(x,v,y_w,y_l)\sim D} \left[ \log \sigma \left( \beta \log \frac{\pi_\theta(y_w|x,v)}{\pi_{\text{ref}}(y_w|x,v)} - \beta \log \frac{\pi_\theta(y_l|x,v)}{\pi_{\text{ref}}(y_l|x,v)} \right) \right] \quad (3)$$

It is demonstrated that DPO assigns equal rewards to all tokens in the responses. When applied to LVLMs for mitigating hallucinations, it lacks emphasis on visual-anchored tokens. Therefore, we propose a novel approach named TPO to mainly solve this problem.

### 3.3 TPO

#### 3.3.1 Visual-Anchored Rewards

We propose a self-calibrated visual-anchored reward generation mechanism based on Equation (2). On the one hand, it can automatically identify visual-anchored tokens in the response during training. On the other hand, it adaptively and iteratively assigns different rewards for tokens according to their visual reliance. The proposed rewards can not only strengthen the attention to visual information for token generation but also align preferences.

To construct the visual-anchored rewards, we first introduce a score  $s$  to measure the visual reliance degree of each token. For this purpose, we add noise into the embedding of the input image  $v$  to obtain the corrupted image  $v_c$ :

$$v_c(k) = \sqrt{\bar{\xi}_k} \cdot v + \sqrt{1 - \bar{\xi}_k} \cdot \epsilon \quad (4)$$

Here, we mainly refer (Zhou et al., 2024a) and set the noise steps  $k = 500$ ,  $\bar{\xi}_k = \prod_{i=0}^k \xi_i$ ,  $\xi$  is a predefined noise parameter derived from a list with 1,000

equally spaced elements.<sup>1</sup> Subsequently, we capture the changes in the probability distribution of each generated token before and after adding noise. For token  $y_i$  of the response  $y$ , the calculation of  $s_{y_i}$  is formulated as Equation (5). Notably, here  $p_{\log}$  refers to the raw logits output of the model, before applying the softmax transformation.

$$s_{y_i} = p_{\log}(y_i|x, v, y_{<i}) - p_{\log}(y_i|x, v_c, y_{<i}) \quad (5)$$

We have shown an example of the distribution of  $s$  before and after training in Figure 1, it is shown that visual-anchored tokens will obtain higher scores. In other words,  $s$  has the ability to reflect the visual relevance of each token  $y_i$ , this also lays the foundation for the ability of our visual-anchored rewards to self-calibrate based on the visual correlation of tokens.

Furthermore, we introduce a self-calibration process to generate the final visual-anchored rewards. This process aims to ensure that positive samples receive higher rewards than negative samples while optimizing the visual relevance of visual-anchored tokens in all responses. Formally, the process is defined as follows, where the sigmoid function  $\text{sigmoid}(\cdot)$  is used for normalization.

$$c_{y_i} = \begin{cases} a + \text{sigmoid}(s_{y_i}) & \text{if } y_i \in y_w \\ a + 1 - \text{sigmoid}(s_{y_i}) & \text{if } y_i \in y_l \end{cases} \quad (6)$$

The calculated  $c_{y_i}$  is adopted as the final reward in TPO, where  $c_{y_i} \in (a, a + 1)$ . In this way,  $c$  and  $s$  are positively correlated for positive examples, whereas for negative ones, the opposite holds true. In particular,  $p(y_i|x, v, y_{<i}) = p(y_i|x, v_c, y_{<i})$ ,

<sup>1</sup>More details can be found in Appendix A.

means that the token does not associate any visual information. In this case, no visual-anchored reward should be assigned for this token. To this end, we set  $a = 0.5$  in Equation (6), so that when  $s = 0, c = 1$ , the rewards will not take effect.

### 3.3.2 Token Preference Optimization

After obtaining the reward  $c_{y_i}$  to  $y_i$ , the output cumulative distribution can be calculated:

$$\pi(y|x, v) = \prod_{y_i \in \mathcal{Y}} c_{y_i} \quad (7)$$

Especially, when  $c_{y_i} = 1$ , the probability of  $y_i$  will not be accumulated. By multiplying the probability distribution with the visual-anchored rewards, we obtain a novel KL-constrained reward maximization objective:

$$\begin{aligned} \max_{\pi} E_{(x,v,y)} \left[ r'(x, v, y) - \beta D_{KL} \left( \left[ \pi_{\theta}(y|x, v) \right. \right. \right. \\ \left. \left. \left. \times \pi_{\theta}^v(y|x, v) \right] \left\| \left[ \pi_{\text{ref}}(y|x, v) \times \pi_{\text{ref}}^v(y|x, v) \right] \right) \right] \end{aligned} \quad (8)$$

Thus, the optimal solution formula for the maximization objective of the KL-constrained reward is as follows:

$$\begin{aligned} \pi_{\theta}(y|x, v) \times \pi_{\theta}^v(y|x, v) = \frac{1}{Z(x)} [\pi_{\text{ref}}(y|x, v) \times \\ \pi_{\text{ref}}^v(y|x, v)] \exp \left( \frac{1}{\beta} r'(x, v, y) \right) \end{aligned} \quad (9)$$

Rearranging the Eq (9), we obtain the new reward function:

$$\begin{aligned} r'(x, v, y) \\ = \beta \log \frac{\pi_{\theta}(y|x, v) \times \pi_{\theta}^v(y|x, v)}{\pi_{\text{ref}}(y|x, v) \times \pi_{\text{ref}}^v(y|x, v)} + \beta Z(x) \\ = \beta \sum_{y_i \in \mathcal{Y}} [\log (p_{\theta}(y_i|x, v, y_{<i}) \cdot c_{\theta}) \\ - \log (p_{\text{ref}}(y_i|x, v, y_{<i}) \cdot c_{\text{ref}})] + \beta Z(x) \\ = \beta \sum_{y_i \in \mathcal{Y}} [\log p_{\theta}(y_i|x, v, y_{<i}) - \\ \log p_{\text{ref}}(y_i|x, v, y_{<i}) + \log \frac{c_{\theta}}{c_{\text{ref}}}] + \beta Z(x) \end{aligned} \quad (10)$$

Compared to the original reward function in DPO (Equation (2)), we multiply each  $p(y_i|x, v, y_{<i})$  by the generated visual-anchored rewards  $c_{y_i}$  at the token level. For  $c_{\theta}$ , its computation is continuously updated at each step during

training as the model changes. In the calculation of each token in the entire reward function, we add a term  $\log \frac{c_{\theta}}{c_{\text{ref}}} \in (-\log 3, \log 3)$ , which has a reasonable upper and lower bound. For positive samples, this term is expected to increase, while for negative samples, it is expected to decrease. Due to the different methods of calculating  $c_{y_i}$  that we set in Equation (6), this will encourage the increase of  $s_{y_i}$  during the training process, making the token generation focus more on visual information.

Thus, following the Bradley-Terry model, when given the positive and negative samples  $\mathcal{D} = \{x^{(i)}, v^{(i)}, y_w^{(i)}, y_l^{(i)}\}_{i=1}^N$ , we obtain our maximum likelihood objective:

$$\begin{aligned} \mathcal{L}_{TPO}(\pi_{\theta}; \pi_{\text{ref}}) = -\mathbb{E}_{(x,v,y_w,y_l) \sim \mathcal{D}} \left[ \log \sigma \right. \\ \left( \beta \log \frac{\pi_{\theta}(y_w|x, v) \times \pi_{\theta}^v(y_w|x, v)}{\pi_{\text{ref}}(y_w|x, v) \times \pi_{\text{ref}}^v(y_w|x, v)} - \right. \\ \left. \beta \log \frac{\pi_{\theta}(y_l|x, v) \times \pi_{\theta}^v(y_l|x, v)}{\pi_{\text{ref}}(y_l|x, v) \times \pi_{\text{ref}}^v(y_l|x, v)} \right) \left. \right] \end{aligned} \quad (11)$$

## 4 Experiment

### 4.1 Setup

Aligning with previous DPO-based approaches on hallucination mitigation, we adopt the popular LVLM, LLaVA-1.5 (Liu et al., 2024b), as the backbone model to validate the effectiveness of our TPO. As for the dataset, we directly utilize the preference pairs provided by RLHF-V (5k) without their fine-grained human annotations.

**Benchmarks:** We primarily conduct the experiments on three hallucination benchmarks: (1) AMBER (Wang et al., 2023): a multi-dimensional hallucination benchmark with over 15k samples. We mainly focus on its discriminative part and report Accuracy and F1 metrics referencing (Yu et al., 2024c); (2) MMHal-Bench (Sun et al., 2023): it measures the hallucination rate and informativeness of responses. (3) HallusionBench (Guan et al., 2024): it evaluates visual illusions and knowledge hallucinations through systematically structured discriminative tasks. We also test the performance on four general evaluation benchmarks: (1) SEED Bench (Li et al., 2023a): a benchmark for LVLMs on generative comprehension. (2) MMBench (Liu et al., 2025): a comprehensive benchmark designed to evaluate the capabilities across various tasks and modalities. (3) LLaVA Bench (Liu et al., 2024c):

Method	AMBER		MMHal		HallusionBench			General Benchmarks			
	Acc	F1	Score	Hall ↓	Easy	Hard	aAcc	SEED	MMB	LLaVA	MM-Vet
LLaVA-1.5-7B	71.7	74.3	2.01	61.46	42.64	41.16	47.21	66.1	<u>73.3</u>	65.6	31.6
+ DPO	<u>77.5</u>	<u>82.1</u>	2.14	58.33	37.36	37.21	43.84	<u>66.4</u>	<u>73.3</u>	<u>69.1</u>	31.6
+ CSR	73.2	76.1	2.05	60.42	<b>43.08</b>	41.16	47.48	65.9	73.0	68.9	31.0
+ POVID	71.9	74.7	<u>2.26</u>	<u>55.21</u>	<u>42.86</u>	41.63	47.56	66.1	73.2	68.2	<u>31.7</u>
+ RLHF-V	74.8	78.5	2.02	60.42	42.20	<u>43.72</u>	48.27	66.1	73.1	68.0	32.3
+ V-DPO	–	81.6	2.16	56.00	–	–	<b>51.63</b>	–	–	–	–
<b>+ TPO (Ours)</b>	<b>79.3</b>	<b>85.0</b>	<b>2.47</b>	<b>51.04</b>	41.76	<b>48.37</b>	<u>50.22</u>	<b>66.6</b>	<b>73.6</b>	<b>70.2</b>	<b>33.0</b>
LLaVA-1.5-13B	71.3	73.1	2.38	53.13	<u>44.40</u>	36.51	46.94	68.2	<u>76.7</u>	<u>73.1</u>	36.1
+ DPO	<u>83.2</u>	<u>86.9</u>	2.47	<u>51.04</u>	<b>45.49</b>	<u>43.49</u>	<u>50.22</u>	<u>68.6</u>	76.6	72.8	<u>37.5</u>
+ RLHF-V	79.2	82.3	<u>2.50</u>	52.08	43.96	40.00	48.27	68.2	<u>76.7</u>	<b>76.7</b>	<b>38.5</b>
<b>+ TPO (Ours)</b>	<b>83.9</b>	<b>88.0</b>	<b>2.72</b>	<b>45.83</b>	<u>44.40</u>	<b>46.05</b>	<b>50.93</b>	<b>68.7</b>	<b>76.8</b>	72.8	36.2

Table 2: Performance of LLaVA-1.5 on hallucination and general benchmarks. Score and Hall refer to the overall GPT-4 score and hallucination rate, respectively. Easy represents the accuracy of with original images, hard represents the accuracy with manually edited challenging images, and aAcc is the average accuracy for each question. The results for POVID (Zhou et al., 2024a) and CSR (Zhou et al., 2024b) are based on our testing of their open-source model weights, while the results for V-DPO (Xie et al., 2024) are taken from previous work. (**bold**: the best score; underline: the second best)

a benchmark for evaluating multi-modal conversation, detailed description, and complex reasoning. (4) MM-Vet (Yu et al., 2023): a benchmark assessing for integrated capabilities.

**Baselines:** In this work, we mainly compare TPO with the SFT model of LLaVA-1.5-7B, as well as with DPO and V-DPO (Xie et al., 2024) methods trained using RLHF-V (Yu et al., 2024b) data, along with two improved methods, CSR (Zhou et al., 2024b) and POVID (Zhou et al., 2024a). Moreover, to evaluate the effectiveness and robustness of TPO as the model size increases, we further compare it with the LLaVA-1.5-13B SFT model, and also against DPO and RLHF-V methods.

## 4.2 Main Results

In Table 2, we present the main results of our TPO and baseline methods. On hallucination benchmarks, our method shows significant improvements over all previous preference learning methods on both the 7B and 13B models. Specifically, compared to the original LLaVA model, we achieve improvements of 20.4% on AMBER F1, 22.8% on MMHAL score, and 8.5% on HallusionBench aAcc at most. This validates the effectiveness of our method in helping the model mitigate hallucination issues and enhance the performance of visual question answering.

Notably, on the HallusionBench evaluation metrics, "Easy" represents the accuracy of original image-based questions, which tend to rely on prior knowledge, while "Hard" represents the accuracy

of questions based on manually edited images, which tend to rely on visual information. Our method leads to the most significant improvement for the original model on hard questions, with a slight improvement on easy questions. This indicates that, compared to other methods, our approach enables the model to focus more on visual information rather than the textual prior knowledge to provide accurate answers.

On general benchmarks, compared to other methods, our approach remains stable against the original LLaVA model and achieves the greatest improvement on most benchmarks. We attribute it to that our method helps the model associate with more visual information when answering questions. This shows that our approach can improve hallucination issues while maintaining good performance on general evaluation tasks.

## 4.3 Ablation Studies

To further demonstrate how our method helps improve model performance by reducing hallucinations, we conduct ablation experiments for the noisy steps, the introduced parameter  $a$ , and the self-calibrated process for rewards. These experiments are performed on LLaVA-1.5-7B consistently with the main experiments, including hallucination and general evaluation benchmarks.

**Noise Steps :** We ablate on the noise steps in Figure 3 (a). As shown, the optimal performance is achieved at the step of 500. This medium corruption enables the model to grasp the general outline

Method	AMBER		MMHal		HallusionBench			General Benchmarks			
	Acc	F1	Score	Hall ↓	Easy	Hard	aAcc	SEED	MMB	LLaVA	MM-Vet
LLaVA-1.5-7B	71.70	74.3	2.01	61.46	42.64	41.16	47.21	66.1	<u>73.3</u>	65.6	31.6
Only Win	79.10	84.5	2.24	56.25	44.62	46.05	<b>50.40</b>	66.6	73.6	69.8	31.7
Only Loss	79.20	84.8	2.33	53.13	42.20	47.91	49.87	66.6	73.5	<b>70.7</b>	32.0
Opposite	75.30	80.7	1.91	64.58	42.42	45.58	48.63	65.6	73.1	68.9	32.1
<b>TPO (Ours)</b>	<b>79.30</b>	<b>85.0</b>	<b>2.47</b>	<b>51.04</b>	<b>41.76</b>	<b>48.37</b>	50.22	<b>66.6</b>	<b>73.6</b>	70.2	<b>33.0</b>

Table 3: Ablation Studies. Performance of LLaVA-1.5 on hallucination and general benchmarks. (**bold**: the best score)

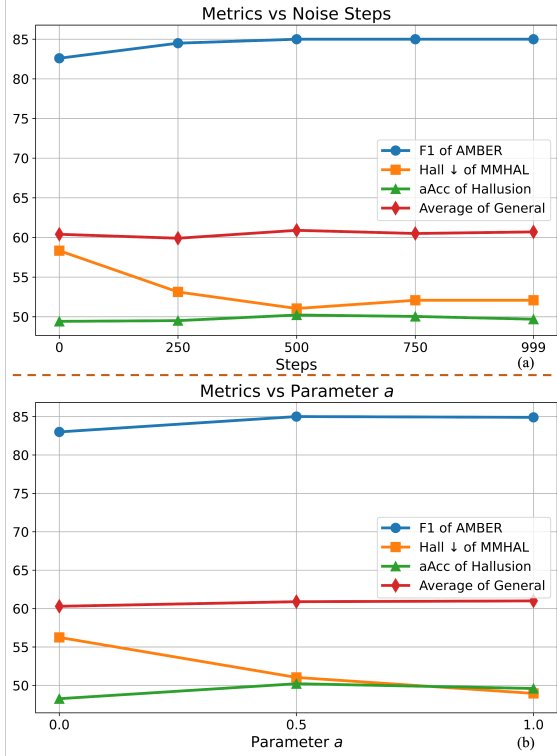


Figure 3: Performance curves with the change of the noise steps-(a) and the change of parameter  $a$ -(b). We separately present the F1 of AMBER, the hallucination rate of MMHAL, the aACC of HallusionBench, and the average value of the general benchmarks. More detailed metrics can be found in the Appendix B.

of the image while missing the detailed contents, which is prone to generate hallucinations of the visual-anchored tokens.

**Parameter  $a$ :** We conduct experiments by varying the parameter  $a$  introduced in Equation (6) with the results shown in Figure 3 (b). By setting  $a = [0, 0.5, 1]$ , we observed consistently good performance across all configurations. This suggests that effective performance is achieved as long as the reward mechanism successfully highlights token differences and identifies visually anchored tokens. Notably, the best overall results are obtained

with  $a = 0.5$ , validating our proposed method and hypothesis. This indicates that when the visual-anchored score  $s = 0$ , setting  $c = 1$ , not introducing additional reward signals can yield better outcomes.

**Visual-Anchored Rewards :** Furthermore, Table 3 demonstrates that TPO can enhance model performance when rewards are assigned separately to positive and negative samples, achieving results comparable to those obtained by rewarding both simultaneously. However, by providing opposite rewards to positive and negative samples, where rewards are negatively correlated with the visual relevance of positive samples and positively correlated with that of negative samples, TPO’s performance significantly deteriorates. In some metrics, this approach yields even poorer results than the original LLaVA-1.5 model. This further underscores the validity of the designation of visual-anchored rewards.

By integrating these selection methods, we achieve superior overall performance, thereby highlighting the value and efficacy of our approach. This integration underscores both the simplicity and effectiveness of our method in achieving robust results.

#### 4.4 Analysis

**Attentions :** To further substantiate the effectiveness of our method in enhancing visual alignment, we visualize the relevance between response and image tokens, both before and after training with TPO. In this statistic, the relevance is quantified using the sum of attention weights. As depicted in Figure 4, post-TPO training, the overall image attention weights for response tokens significantly increase, especially for visual-anchored tokens (e.g., table, cord). This underscores our method’s efficacy in improving the model’s capacity to integrate visual information during response generation, thus mitigating the hallucination issue.

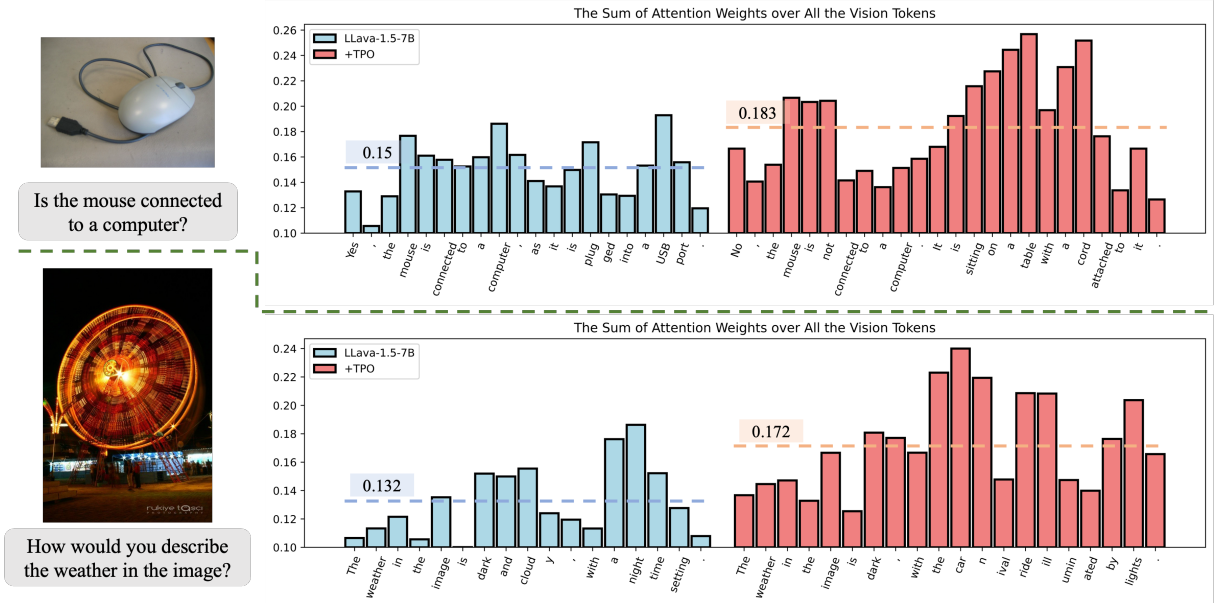


Figure 4: Comparison of attention weights for LLaVA-1.5 before and after TPO training. Each horizontal line represents the mean of that data set. The blue section on the left response incorrectly, with many 'visual-anchored tokens' tokens having high attention weights but resulting in hallucinated responses (e.g. USB, cloud). The red section on the right answered correctly.

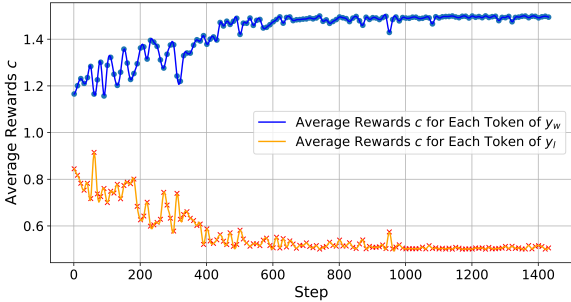


Figure 5: The curve of changes in self-calibrated rewards for positive and negative samples over training steps, with a sample point taken every 10 steps.

**Self-Calibration :** To illustrate that our method enables the model to progressively enhance its focus on visual information through continuous self-calibration during training, we present the evolution of scores for positive and negative samples, as calculated by Equation (6), across various training steps. With  $a = 0.5$ , it follows that  $c_{y_i} \in (0.5, 1.5)$ . As shown in Figure 5, the scores for positive samples gradually approach their maximum values, while those for negative samples approach their minimum values, indicating convergence. This trend illustrates the self-calibrating effect of our method, which ultimately enhances the model's ability to focus on visual information.

## 5 Conclusion

In this study, we propose TPO, a novel token preference optimization framework, aimed at mitigating hallucinations in LLMs. TPO incorporates a self-calibrated visual-anchored reward mechanism that automatically identifies "vision-anchored tokens" and adaptively assigns appropriate rewards to them. By adding noise to the visual input and capturing changes in the generation probability of each token, TPO computes a score indicating each token's relevance to visual information. Subsequently, a self-calibration process adjusts these scores to ensure that: 1) Rewards for positive examples exceed those for negative examples. 2) The final rewards enhance the focus on visual information for all of "vision-anchored tokens" in preference data. Based on the self-calibrated visual-anchored reward, TPO can perform more efficient token-level preference alignment optimization for LLMs. Experimental results have proved that TPO not only alleviates the hallucination problem but also strengthens the model's attention to visual input when generating responses.

## 6 Limitation

Although our method has achieved outstanding performance in addressing the hallucination problem, the self-calibrated visual-anchored rewards



approach we used in this paper can be extended to even broader areas. By altering the way noise is added to images, we can shift from adding noise to the entire image to adding noise to specific key objects. It can enable the model to specifically improve its focus on image information in certain domains, thus having extensive industrial applications. We will continue to expand in this direction, and we believe that the technology we have proposed in this paper has a vast space for further development and application.

## 7 Ethic Statement

The main purpose of this article is to alleviate the hallucination problem in LVLM using reinforcement learning method. By employing a self-calibrated visual-anchored reward approach, we propose the TPO method, which significantly addresses the hallucination issue and helps the model connect with more visual information. All the models and datasets we used are open source, so we believe that the work in this paper does not pose any potential threats.

## References

- Jinze Bai, Shuai Bai, Shusheng Yang, Shijie Wang, Sinan Tan, Peng Wang, Junyang Lin, Chang Zhou, and Jingren Zhou. 2023. Qwen-vl: A frontier large vision-language model with versatile abilities. *arXiv preprint arXiv:2308.12966*.
- Zechen Bai, Pichao Wang, Tianjun Xiao, Tong He, Zongbo Han, Zheng Zhang, and Mike Zheng Shou. 2024. Hallucination of multimodal large language models: A survey. *arXiv preprint arXiv:2404.18930*.
- Ralph Allan Bradley and Milton E Terry. 1952. Rank analysis of incomplete block designs: I. the method of paired comparisons. *Biometrika*, 39(3/4):324–345.
- Zhaorun Chen, Zhuokai Zhao, Hongyin Luo, Huaxiu Yao, Bo Li, and Jiawei Zhou. 2024. Halc: Object hallucination reduction via adaptive focal-contrast decoding. *arXiv preprint arXiv:2403.00425*.
- Tianrui Guan, Fuxiao Liu, Xiyang Wu, Ruiqi Xian, Zongxia Li, Xiaoyu Liu, Xijun Wang, Lichang Chen, Furong Huang, Yaser Yacoob, et al. 2024. Hallusionbench: an advanced diagnostic suite for entangled language hallucination and visual illusion in large vision-language models. In *Proceedings of the IEEE/CVF Conference on Computer Vision and Pattern Recognition*, pages 14375–14385.
- Zongbo Han, Zechen Bai, Haiyang Mei, Qianli Xu, Changqing Zhang, and Mike Zheng Shou. 2024. Skip\n: A simple method to reduce hallucination in large vision-language models. *arXiv preprint arXiv:2402.01345*.
- Qidong Huang, Xiaoyi Dong, Pan Zhang, Bin Wang, Conghui He, Jiaqi Wang, Dahua Lin, Weiming Zhang, and Nenghai Yu. 2024. Opera: Alleviating hallucination in multi-modal large language models via over-trust penalty and retrospection-allocation. In *Proceedings of the IEEE/CVF Conference on Computer Vision and Pattern Recognition*, pages 13418–13427.
- Aaron Hurst, Adam Lerer, Adam P Goucher, Adam Perelman, Aditya Ramesh, Aidan Clark, AJ Ostrow, Akila Welihinda, Alan Hayes, Alec Radford, et al. 2024. Gpt-4o system card. *arXiv preprint arXiv:2410.21276*.
- Seongyun Lee, Sue Hyun Park, Yongrae Jo, and Minjoon Seo. 2023. Volcano: mitigating multimodal hallucination through self-feedback guided revision. *arXiv preprint arXiv:2311.07362*.
- Sicong Leng, Hang Zhang, Guanzheng Chen, Xin Li, Shijian Lu, Chunyan Miao, and Lidong Bing. 2024. Mitigating object hallucinations in large vision-language models through visual contrastive decoding. In *Proceedings of the IEEE/CVF Conference on Computer Vision and Pattern Recognition*, pages 13872–13882.
- Bohao Li, Rui Wang, Guangzhi Wang, Yuying Ge, Yixiao Ge, and Ying Shan. 2023a. Seed-bench: Benchmarking multimodal llms with generative comprehension. *arXiv preprint arXiv:2307.16125*.
- Junnan Li, Dongxu Li, Silvio Savarese, and Steven Hoi. 2023b. Blip-2: Bootstrapping language-image pre-training with frozen image encoders and large language models. In *International conference on machine learning*, pages 19730–19742. PMLR.
- Fuxiao Liu, Kevin Lin, Linjie Li, Jianfeng Wang, Yaser Yacoob, and Lijuan Wang. 2023. Mitigating hallucination in large multi-modal models via robust instruction tuning. In *The Twelfth International Conference on Learning Representations*.
- Hanchao Liu, Wenyuan Xue, Yifei Chen, Dapeng Chen, Xiutian Zhao, Ke Wang, Liping Hou, Rongjun Li, and Wei Peng. 2024a. A survey on hallucination in large vision-language models. *arXiv preprint arXiv:2402.00253*.
- Haotian Liu, Chunyuan Li, Yuheng Li, and Yong Jae Lee. 2024b. Improved baselines with visual instruction tuning. In *Proceedings of the IEEE/CVF Conference on Computer Vision and Pattern Recognition*, pages 26296–26306.
- Haotian Liu, Chunyuan Li, Qingyang Wu, and Yong Jae Lee. 2024c. Visual instruction tuning. *Advances in neural information processing systems*, 36.

- Yuan Liu, Haodong Duan, Yuanhan Zhang, Bo Li, Songyang Zhang, Wangbo Zhao, Yike Yuan, Jiaqi Wang, Conghui He, Ziwei Liu, et al. 2025. Mm-bench: Is your multi-modal model an all-around player? In *European Conference on Computer Vision*, pages 216–233. Springer.
- Alec Radford, Jong Wook Kim, Chris Hallacy, Aditya Ramesh, Gabriel Goh, Sandhini Agarwal, Girish Sastry, Amanda Askell, Pamela Mishkin, Jack Clark, et al. 2021. Learning transferable visual models from natural language supervision. In *International conference on machine learning*, pages 8748–8763. PMLR.
- Rafael Rafailov, Archit Sharma, Eric Mitchell, Christopher D Manning, Stefano Ermon, and Chelsea Finn. 2024. Direct preference optimization: Your language model is secretly a reward model. *Advances in Neural Information Processing Systems*, 36.
- Hao Shao, Shengju Qian, Han Xiao, Guanglu Song, Zhuofan Zong, Letian Wang, Yu Liu, and Hongsheng Li. 2024. Visual cot: Unleashing chain-of-thought reasoning in multi-modal language models. *arXiv preprint arXiv:2403.16999*.
- Zhiqing Sun, Sheng Shen, Shengcao Cao, Haotian Liu, Chunyuan Li, Yikang Shen, Chuang Gan, Liang-Yan Gui, Yu-Xiong Wang, Yiming Yang, et al. 2023. Aligning large multimodal models with factually augmented rlhf. *arXiv preprint arXiv:2309.14525*.
- Gemini Team, Rohan Anil, Sebastian Borgeaud, Jean-Baptiste Alayrac, Jiahui Yu, Radu Soricut, Johan Schalkwyk, Andrew M Dai, Anja Hauth, Katie Millican, et al. 2023. Gemini: a family of highly capable multimodal models. *arXiv preprint arXiv:2312.11805*.
- Junyang Wang, Yuhang Wang, Guohai Xu, Jing Zhang, Yukai Gu, Haitao Jia, Ming Yan, Ji Zhang, and Jitao Sang. 2023. An llm-free multi-dimensional benchmark for mllms hallucination evaluation. *arXiv preprint arXiv:2311.07397*.
- Peng Xia, Kangyu Zhu, Haoran Li, Hongtu Zhu, Yun Li, Gang Li, Linjun Zhang, and Huaxiu Yao. 2024. Rule: Reliable multimodal rag for factuality in medical vision language models. In *Proceedings of the 2024 Conference on Empirical Methods in Natural Language Processing*, pages 1081–1093.
- Yuxi Xie, Guanzhen Li, Xiao Xu, and Min-Yen Kan. 2024. V-dpo: Mitigating hallucination in large vision language models via vision-guided direct preference optimization. *arXiv preprint arXiv:2411.02712*.
- Zhengyuan Yang, Linjie Li, Kevin Lin, Jianfeng Wang, Chung-Ching Lin, Zicheng Liu, and Lijuan Wang. 2023. The dawn of lmms: Preliminary explorations with gpt-4v (ision). *arXiv preprint arXiv:2309.17421*, 9(1):1.
- Shukang Yin, Chaoyou Fu, Sirui Zhao, Tong Xu, Hao Wang, Dianbo Sui, Yunhang Shen, Ke Li, Xing Sun, and Enhong Chen. 2023. Woodpecker: Hallucination correction for multimodal large language models. *arXiv preprint arXiv:2310.16045*.
- Qifan Yu, Juncheng Li, Longhui Wei, Liang Pang, Wentao Ye, Bosheng Qin, Siliang Tang, Qi Tian, and Yueting Zhuang. 2024a. Hallucidoctor: Mitigating hallucinatory toxicity in visual instruction data. In *Proceedings of the IEEE/CVF Conference on Computer Vision and Pattern Recognition*, pages 12944–12953.
- Tianyu Yu, Yuan Yao, Haoye Zhang, Taiwen He, Yifeng Han, Ganqu Cui, Jinyi Hu, Zhiyuan Liu, Hai-Tao Zheng, Maosong Sun, et al. 2024b. Rlhf-v: Towards trustworthy mllms via behavior alignment from fine-grained correctional human feedback. In *Proceedings of the IEEE/CVF Conference on Computer Vision and Pattern Recognition*, pages 13807–13816.
- Tianyu Yu, Haoye Zhang, Yuan Yao, Yunkai Dang, Da Chen, Xiaoman Lu, Ganqu Cui, Taiwen He, Zhiyuan Liu, Tat-Seng Chua, et al. 2024c. Rlaif-v: Aligning mllms through open-source ai feedback for super gpt-4v trustworthiness. *arXiv preprint arXiv:2405.17220*.
- Weihao Yu, Zhengyuan Yang, Linjie Li, Jianfeng Wang, Kevin Lin, Zicheng Liu, Xinchao Wang, and Lijuan Wang. 2023. Mm-vet: Evaluating large multimodal models for integrated capabilities. *arXiv preprint arXiv:2308.02490*.
- Bohan Zhai, Shijia Yang, Chenfeng Xu, Sheng Shen, Kurt Keutzer, and Manling Li. 2023. Halle-switch: Controlling object hallucination in large vision language models. *arXiv e-prints*, pages arXiv–2310.
- Jiacheng Zhang, Yang Jiao, Shaoxiang Chen, Jingjing Chen, and Yu-Gang Jiang. 2024. Eventhallusion: Diagnosing event hallucinations in video llms. *arXiv preprint arXiv:2409.16597*.
- Yiyang Zhou, Chenhang Cui, Rafael Rafailov, Chelsea Finn, and Huaxiu Yao. 2024a. Aligning modalities in vision large language models via preference fine-tuning. *arXiv preprint arXiv:2402.11411*.
- Yiyang Zhou, Chenhang Cui, Jaehong Yoon, Linjun Zhang, Zhun Deng, Chelsea Finn, Mohit Bansal, and Huaxiu Yao. 2023. Analyzing and mitigating object hallucination in large vision-language models. *arXiv preprint arXiv:2310.00754*.
- Yiyang Zhou, Zhiyuan Fan, Dongjie Cheng, Sihan Yang, Zhaorun Chen, Chenhang Cui, Xiyao Wang, Yun Li, Linjun Zhang, and Huaxiu Yao. 2024b. Calibrated self-rewarding vision language models. *arXiv preprint arXiv:2405.14622*.
- Deyao Zhu, Jun Chen, Xiaoqian Shen, Xiang Li, and Mohamed Elhoseiny. 2023. Minigt-4: Enhancing vision-language understanding with advanced large language models. *arXiv preprint arXiv:2304.10592*.

Method	AMBER		MMHal		HallusionBench			General Benchmarks			
	Acc	F1	Score	Hall ↓	Easy	Hard	aAcc	SEED	MMB	LLaVA	MM-Vet
LLaVA-1.5-7B	71.7	74.3	2.01	61.46	42.64	41.16	47.21	66.1	<u>73.3</u>	65.6	31.6
0 setp	77.6	82.6	2.10	58.33	<b>44.40</b>	45.35	49.42	66.2	73.2	69.9	32.1
250 steps	79.0	84.5	2.33	53.13	43.52	46.05	49.51	66.6	73.4	68.5	31.3
750 steps	79.30	85.0	2.40	52.08	41.76	48.14	50.04	<b>66.7</b>	73.5	69.2	32.8
999 steps	79.20	85.0	2.41	52.08	41.76	47.67	49.69	<b>66.7</b>	73.5	69.2	<b>33.3</b>
<b>500 steps (Ours)</b>	<b>79.30</b>	<b>85.0</b>	<b>2.47</b>	<b>51.04</b>	41.76	<b>48.37</b>	<b>50.22</b>	66.6	<b>73.6</b>	<b>70.2</b>	33.0

Table 4: Detail of Figure 3 (a). (bold: the best score)

Method	AMBER		MMHal		HallusionBench			General Benchmarks			
	Acc	F1	Score	Hall ↓	Easy	Hard	aAcc	SEED	MMB	LLaVA	MM-Vet
LLaVA-1.5-7B	71.7	74.3	2.01	61.46	42.64	41.16	47.21	66.1	<u>73.3</u>	65.6	31.6
$a = 0$	79.2	83.0	2.24	56.25	<b>42.20</b>	43.72	48.27	66.6	73.5	68.4	32.8
$a = 1$	79.2	84.9	2.44	<b>48.96</b>	41.54	47.44	49.60	<b>66.7</b>	<b>73.6</b>	<b>70.8</b>	<b>33.1</b>
$a = 0.5$ (Ours)	<b>79.3</b>	<b>85.0</b>	<b>2.47</b>	51.04	41.76	<b>48.37</b>	<b>50.22</b>	66.6	<b>73.6</b>	70.2	33.0

Table 5: Detail of Figure 3 (b). (bold: the best score)

## A Setup Details

In our experiments, we trained the LLaVA-v1.5 model. For our TPO method and the vanilla DPO method, we set the maximum learning rate to  $5e-8$  on the 7B version and trained for 4 epochs. We set the maximum learning rate to  $2e-7$  on the 7B version and trained for 4 epochs. The RLHF-V training was set according to the paper (Yu et al., 2024b). All parts requiring GPT-4 evaluation use the GPT-4-0613 version, and the MM-Vet testing is conducted on the official evaluation website.

Our experiments were all conducted on a server equipped with 8 GPUs; in specific cases (such as the 13B model), we utilized 32 GPUs. For the hyperparameter setting, all hyperparameters are consistent with those of our main experiment. Moreover, the level of diffusion noise in our model is represented by a formula  $\xi = Sigmoid(l_t) \times (0.5 \times 10^{-2} - 10^{-5}) + 10^{-5}$ , where  $l_t$  is a list of 1,000 numbers taken at equal intervals over the interval  $[-6, 6]$ .

The cases in Figure 1 and Figure 4 come from benchmarks (Sun et al., 2023), while the cases in Figure 2 come from the RLHFV training set (Yu et al., 2024b).

## B Experimental Results

In this section, we will provide a detailed presentation of further ablation studies on the noise steps and  $a$  in Eq 6, as shown in Table 4 and Table 5. The optimal performance for noise steps is attained

at the 500-steps. This level of medium corruption allows the model to capture the general outline of the image while neglecting finer details, which can lead to the generation of hallucinations in the visual-anchored tokens. and The Optimal performance for  $a$  is 0.5, when the visual-anchored score  $s = 0$ , we get  $c = 1$ , not introducing additional reward signals can yield better outcomes.